Vickers, A.C., et al., 2020, Similar Holocene glaciation histories in tropical South America and Africa: Geology, v. 49, https://doi.org/10.1130/G48059.1

Supplementary Material for

"Similar Holocene glaciation histories in tropical South America and Africa"

Cosmogenic Measurements

We measured ^{14}C and ^{10}Be concentrations in all recently deglaciated bedrock samples, and ^{10}Be only in the two samples down valley from the Quelccaya Ice Cap. ^{14}C extraction for all samples was conducted at Tulane University following the methods of Goehring et al. (2019). ^{10}Be was isolated using standard successive anion-cation exchange chromatography from the Quelccaya samples at Tulane University and from the Rwenzori samples at Dartmouth College. Isotopic ratios were measured at Lawrence Livermore Center for Accelerator Mass Spectrometry (^{10}Be) and Woods Hole National Ocean Sciences Accelerator Mass Spectrometry facility (^{14}C). We report conservative ^{14}C uncertainties based on an estimate of long-term lab precision (5.6%; (Goehring et al., 2019) from replicate measurements of the CRONUS-A intercomparison material. ^{10}Be results from the three Rwenzori headwall samples were previously reported in Jackson et al. (2020).

Numerical Model

We developed a numerical model to simulate nuclide production, decay, and erosion to test possible glacier histories that yield cosmogenic nuclide concentrations and ratios in agreement with the measured values for each sample. The model simulates a bedrock depth profile of ^{10}Be and ^{14}C concentrations through time for various exposure scenarios, driving production when exposed, and decay and erosion when ice covered. We assume that ice is thick enough during intervals of burial that production is negligible (>10 m; (Goehring et al., 2011). Production and decay rates are fixed, but erosion rates are systematically adjusted to explore a range of possibilities for each exposure scenario. Production rate profiles are derived from the University of Washington online cosmogenic calculator v3 (Balco et al., 2008) using the LSDn scaling scheme (Lifton et al., 2014) with the global production rate calibration dataset as well as the regional Quelccaya calibration (Kelly et al., 2015). The evolution of nuclide

concentrations in a bedrock column are then driven by a prescribed exposure/erosion scenario in 100-year time steps via equation 1.

$$N(z,t) = P_{NT}(z) \cdot t + N(z,t-1) \cdot e^{(-\lambda_N \cdot t)} \quad (1)$$

Where N is the concentration of the nuclide in the bedrock as a function of depth (z) and time (t), P_{NT} is the total production of the nuclide via spallation and muon production as a function of depth, and λ_N is the decay constant of the nuclide. During times of exposure, the model uses the production portion of equation 1 (left of the addition sign). During times of burial, the model only uses the decay portion of equation 1 (right of the addition sign). Erosion is incorporated by redefining the "surface" as some depth below the top of the bedrock. The model assumes that erosion only takes place during times of burial.

100,000 unique exposure/burial scenarios were randomly generated with the intent to sample a wide range of Holocene histories (Fig. S3). For a given scenario, each time step was assigned exposure or burial based on a specified probability (P) that it would match the designation (exposure or burial) of the previous time step. For example, in a scenario with P = 0.8, each time step has an 80% probability of having the same designation (exposure or burial) as the previous time step. P ranged from 0.6 to 0.99 across the 100,000 scenarios to ensure that exposure and burial intervals fluctuate over a wide range of frequencies (e.g., scenarios with P = 0.6 tend to have more high frequency variability, scenarios with P = 0.99 tend to have more extended intervals of exposure and burial). The model tested erosion rates of 0 to 2500 mm/kyr (in steps of 10 mm/kyr) for the Quelccaya Ice Cap samples and 0 to 200 mm/kyr (in steps of 10 mm/kyr) for the Rwenzori Mountain samples with each scenario. These ranges were selected based on several trial runs of the model.

Each sample was stepped through each exposure scenario (trying all erosion rates) individually, and the scenario was saved if the final surface ^{14}C and ^{10}Be concentrations were within 3σ uncertainty of the sample concentration, including both measurement and production rate (7.3% for ^{14}C and 8.3% for ^{10}Be, 1σ; Borchers et al., 2016) uncertainties, added in quadrature. Scenarios that successfully simulate all samples were considered plausible Holocene histories, and include 2,342 scenarios for Quelccaya and

1,820 scenarios for the Rwenzori (Fig. S4 and 5). Note that the choice of production rate calibration dataset for either nuclide has little bearing on the accepted model simulations (Fig. S4).

All model codes are available in the supplement.

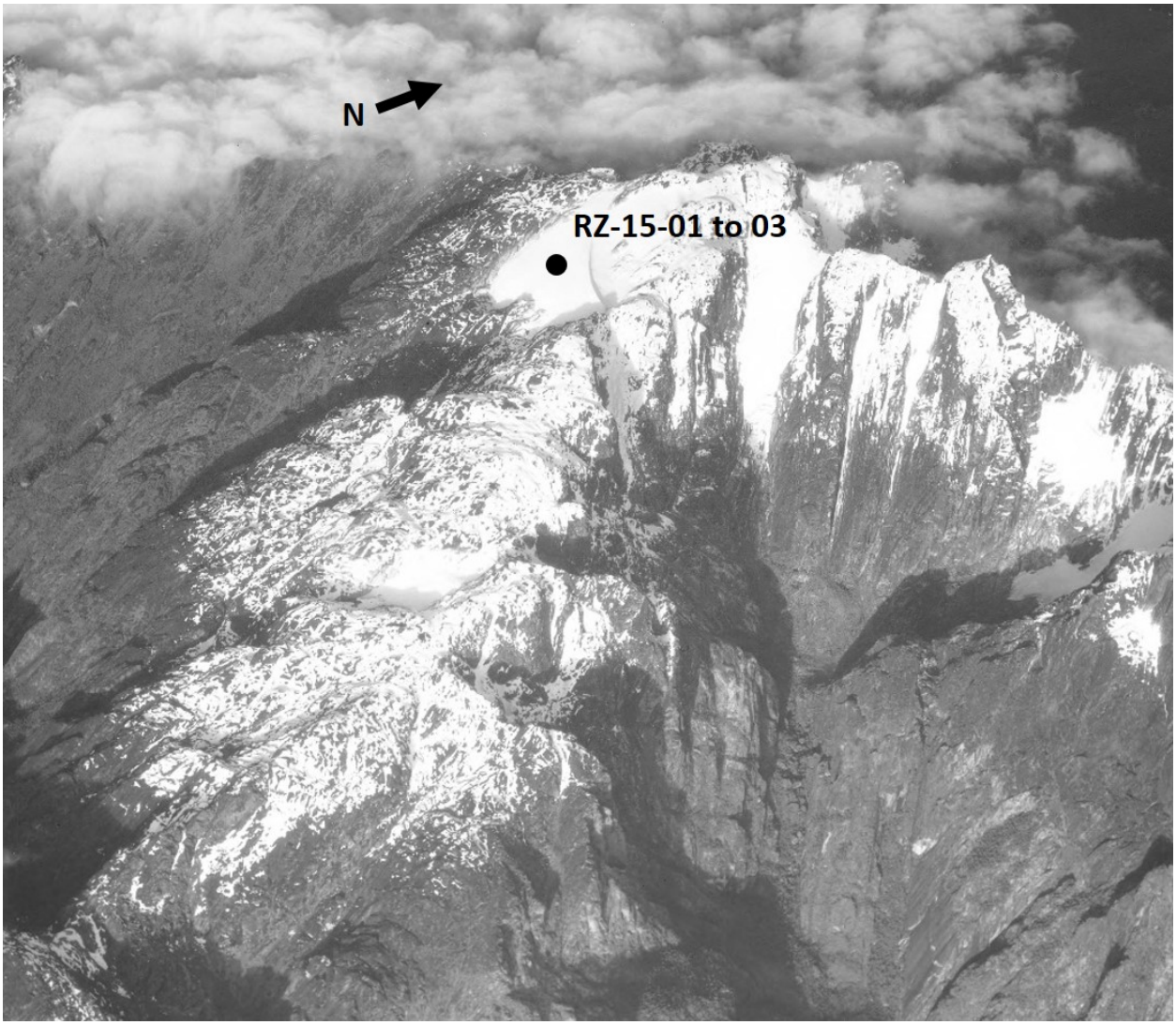

Figure S1. Aerial photo of Weismann's Peak, Rwenzori Mountains, from 1937. Bedrock samples RZ-15-01 to 03 used for this study are covered by ice at the time the photo was taken. These samples have since been exposed and the peak is now ice free.

(photo from https://collections.lib.uwm.edu/digital/collection/agsafrica/id/358/rec/102)

Figure S2. Photos of recently deglaciated bedrock samples from the Quelccaya Ice Cap (blue) and Rwenzori Mountains (red).

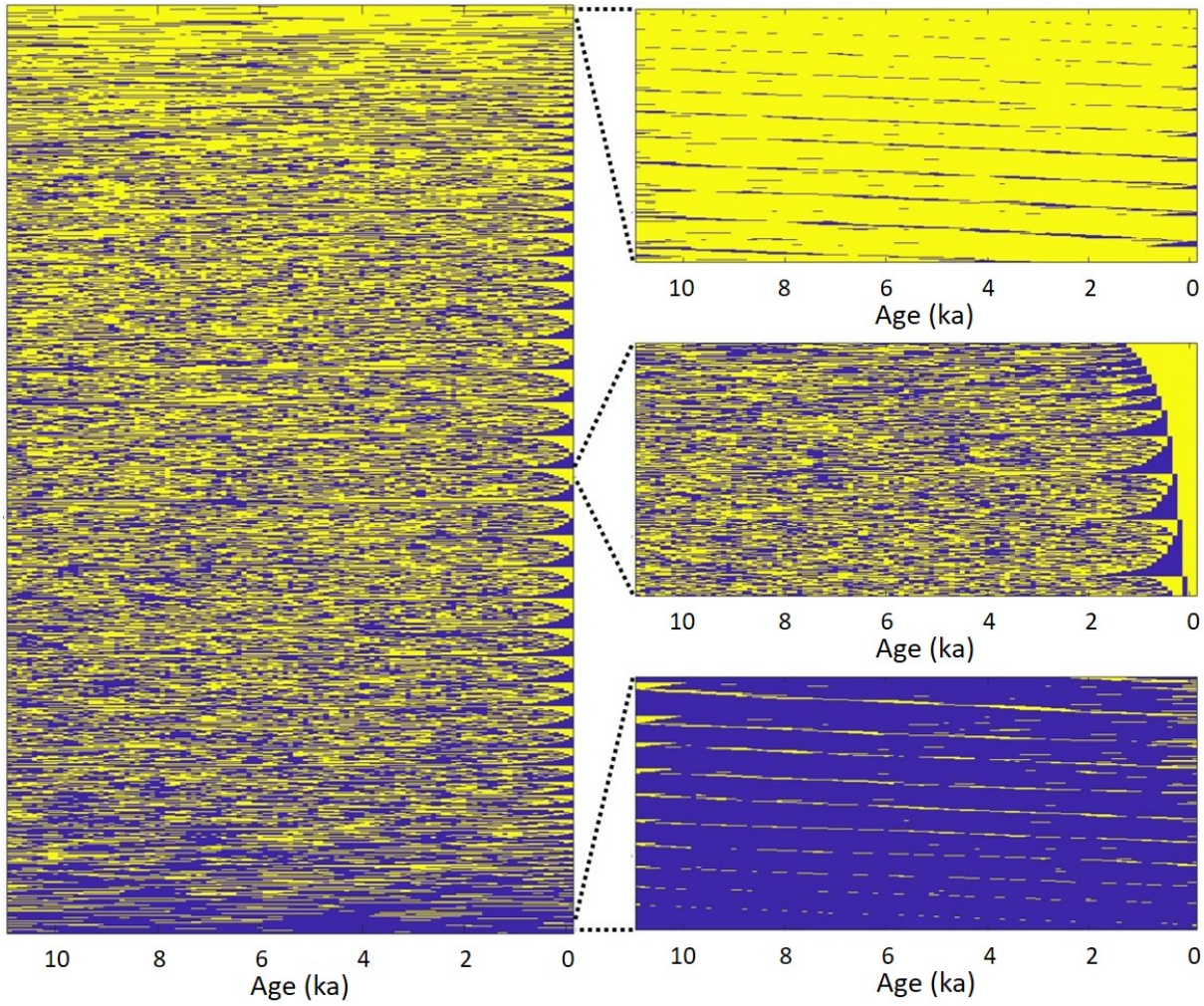

Figure S3. (left) Graphical depiction of all modeled Holocene exposure scenarios (n=100,000), sorted from scenarios with most to least total exposure. Yellow indicates periods of exposure (glacier is smaller than today); blue indicates periods of burial (glacier is larger than today). Each horizontal line represents a single scenario. (right) Zoom-in of 1000 simulations with (top) the most total exposure, (middle) an intermediate amount of exposure, and (bottom) the least total exposure.

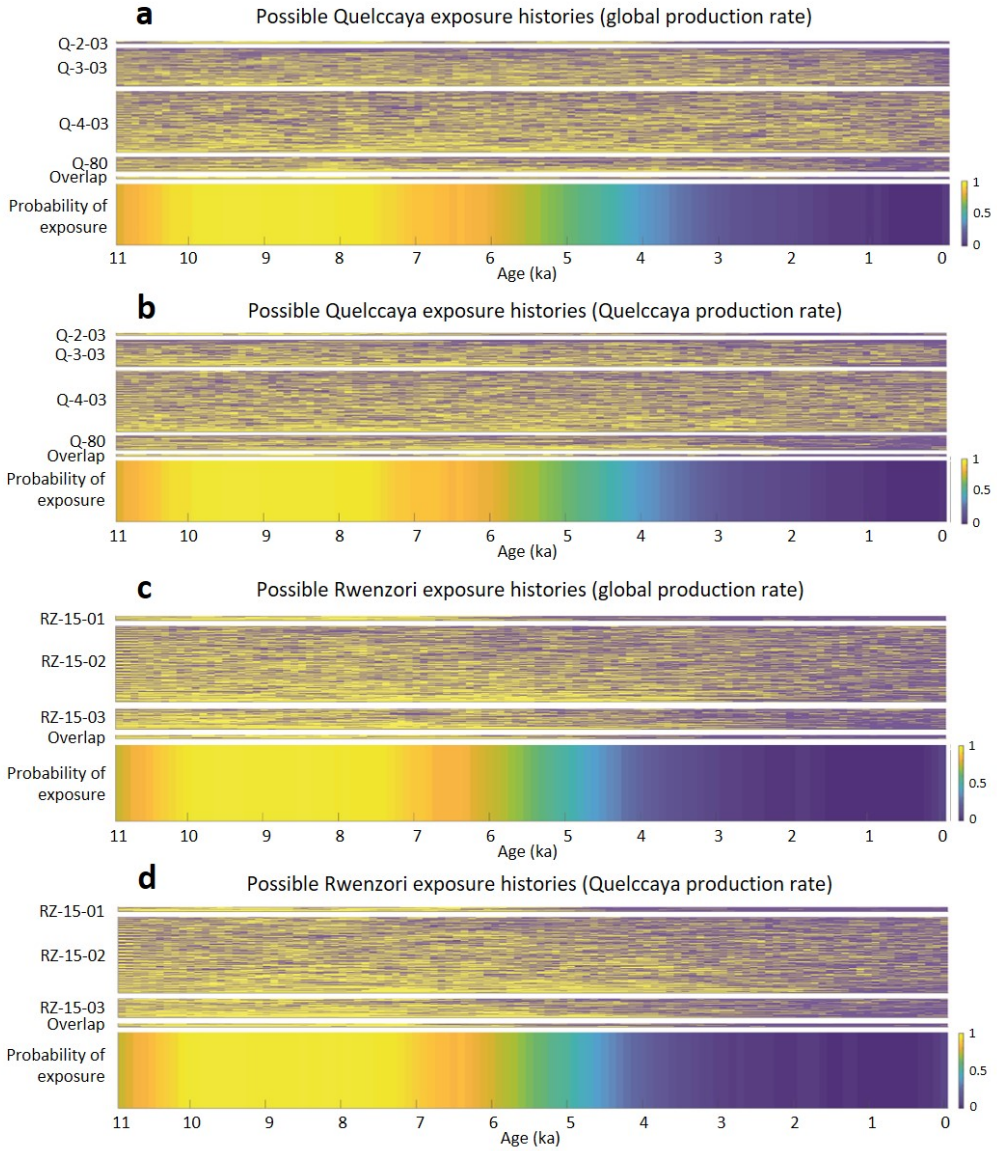

Figure S4. Exposure scenarios that yield ^{14}C and ^{10}Be concentrations within 3σ uncertainty of the (**a, b**) Quelccaya Ice Cap and (**c, d**) Rwenzori Mountains samples using nuclide production rates from the (**a, c**) global and (**b, d**) Quelccaya (Kelly et al., 2015) calibration datasets. Yellow indicates periods of exposure (glacier is smaller than today); blue indicates periods of burial (glacier is larger than today). Each horizontal line is a separate scenario. Panels show scenarios consistent with each sample individually (labeled next to each panel) as well as all of the samples ("Overlap"), and the shaded lowermost panels show the proportion of scenarios with exposure in each time step from the Overlap panels.

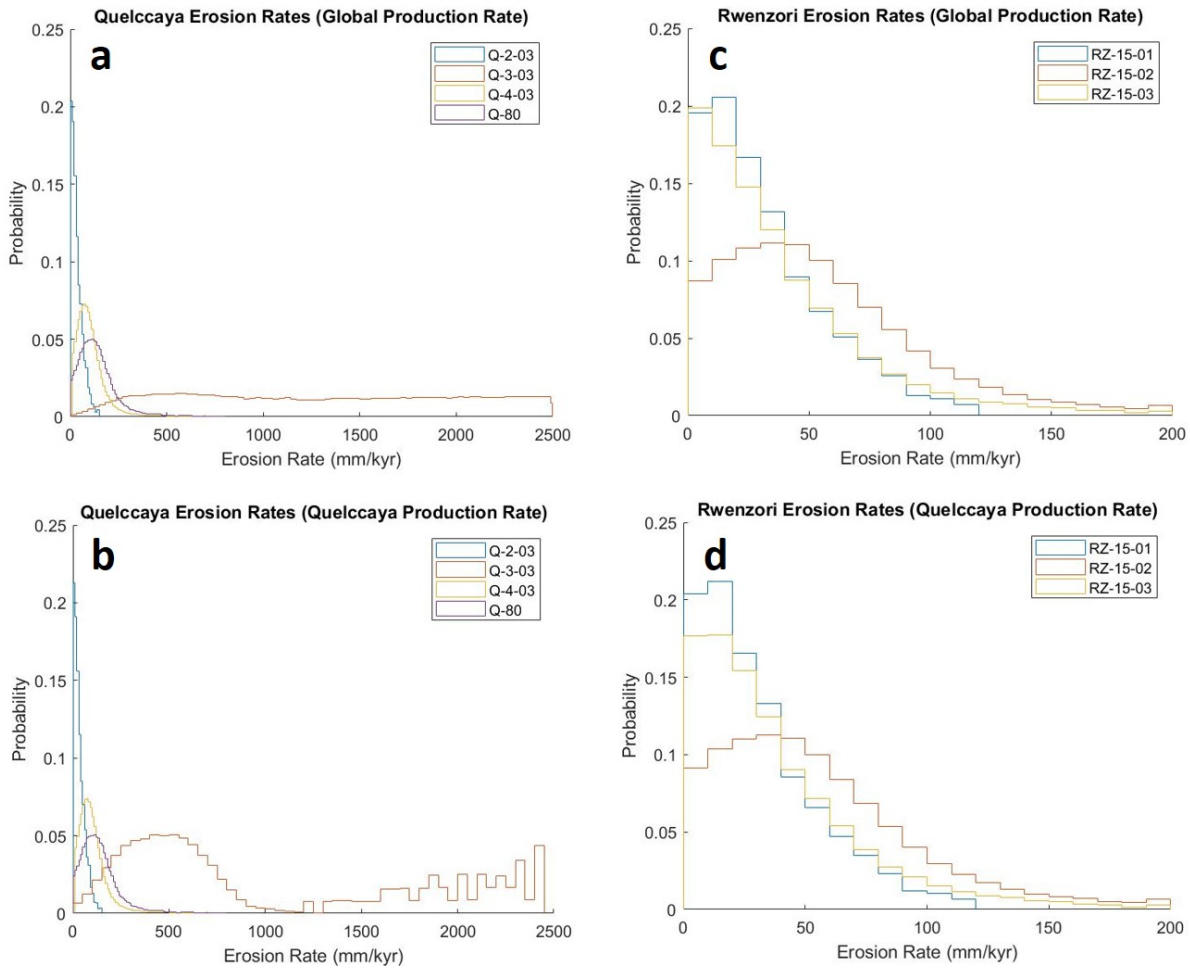

Figure S5. Simulated erosion rates for successful exposure scenarios for the (**a, b**) Quelccaya Ice Cap and (**c, d**) Rwenzori Mountains samples using nuclide production rates from the (**a, c**) global and (**b, d**) Quelccaya (Kelly et al., 2015) calibration datasets.

Table S1. ^{10}Be and ^{14}C sample data. All uncertainties are 1σ.

Sample	Lat (DD)	Lon (DD)	Elev (m asl)	Thickness (cm)	Shielding	^{10}Be[1] (10^4 atoms/g)	^{14}C[1] (10^4 atoms/g)	^{10}Be age[2] (yr)	^{14}C age[2] (yr)	^{14}C/^{10}Be
Rwenzori Mountains										
RZ-15-01	0.32793	29.88877	4509	1.9	0.969	16.57±0.18	13.81±0.77	5323±58	1702±106	0.83±0.05
RZ-15-02	0.32786	29.88887	4526	1.4	0.97	16.89±0.18	18.09±1.01	5346±58	2346±152	1.07±0.06
RZ-15-03	0.32781	29.88871	4536	2.8	0.97	18.89±0.17	18.13±1.02	5827±52	2370±154	0.96±0.05
Quelccaya Ice Cap										
Q-2-03	-13.9299	-70.8531	5225	3.0	0.969	25.62±0.57	21.92±1.23	5656±126	1992±126	0.86±0.05
Q-3-03	-13.93	-70.8526	5210	5.0	0.995	1.80±0.12	2.56±0.71	392±26	198±14	1.42±0.41
Q-4-03	-13.9298	-70.853	5220	4.0	0.995	21.69±0.43	26.75±1.50	4904±98	2557±168	1.23±0.07
Q-80	-13.9327	-70.8537	5196	3.0	0.996	12.08±0.28	13.86±0.78	2824±65	1156±69	1.15±0.07
Q-81	-13.9332	-70.8567	5225	3.0	0.997	56.00±1.34	20.26±1.14	10970±263	1768±110	0.36±0.02
Q-74	-13.909	-70.8747	5032	2.0	0.997	51.59±0.99	-	10920±210	-	-
Q-75	-13.909	-70.8747	5034	2.0	0.997	52.05±1.00	-	10975±211	-	-

[1]Corrected for background ^{14}C and ^{10}Be. See Tables S3 and S4 for background measurements.
[2]Calculated using the CRONUS-Earth online calculator v.3 (Balco et al., 2008) with the LSDn scaling scheme (Lifton et al., 2014) and global production rate. Ages assume continuous exposure with no erosion. Uncertainties are analytical (i.e., internal) only.

Table S2. ^{10}Be sample data details. All uncertainties are 1σ.

Sample	Be Carrier	^{9}Be Carrier	^{10}Be/^{9}Be[1]	Quartz Mass	^{10}Be Blank

	Added (g)	Concentration (ppm)	(10^{-13})	(g)	
Rwenzori Mountains					
RZ-15-01	0.0961	1337	19.4±0.21	100.5702	MJ-BL65
RZ-15-02	0.0967	1337	19.7±0.22	100.7899	MJ-BL65
RZ-15-03	0.0930	1337	23.0±0.20	101.3296	MJ-BL65
Quelccaya Ice Cap					
Q-2-03	0.2601	1040	2.92±0.05	20.0666	BAB_061517
Q-3-03	0.2601	1040	0.28±0.01	20.0336	BAB_061517
Q-4-03	0.2601	1040	2.24±0.04	18.0134	BAB_061517
Q-80	0.2601	1040	1.44±0.03	20.3979	BAB_061517
Q-81	0.2607	1040	6.27±0.13	20.0366	BAB_061517
Q-74	0.2030	996	2.62±0.05	6.8736	MKBL1_Nov07 and MKBL2_Nov07
Q-75	0.2047	996	2.49±0.05	6.4334	MKBL1_Nov07 and MKBL2_Nov07

[1]Measured relative to standard 07KNSTD3110 with an assumed $^{10}Be/^{9}Be$ ratio of 2.85×10^{-12} (Nishiizumi et al., 2007).

Table S3. ^{14}C sample data details. All uncertainties are 1σ.

Sample ID	Quartz Mass (g)	C Yield (µg)	Diluted C Mass (µg)	$^{14}C/^{13}C$ (10^{-10}) *graphitization corrected	$\delta^{13}C$	$^{14}C/C$ (10^{-13})	Blank Corrected ^{14}C[1] (10^5 atoms)	^{14}C[1] (10^4 atoms/g)	Eff. Blank (atoms) (10^4)
Rwenzori Mountains									
RZ-15-01	5.0125	9.7±0.1	104.2±1.3	13.74±0.00009675	-4.56±2.52	10.507 ±0.00110	6.922±0.388	13.81±0.77	9.533±0.5947
RZ-15-02	4.9938	11.5±0.1	103.9±1.3	17.49±0.00008598	-5.48±2.22	1.917±0.001003	9.036±0.506	18.09±1.01	9.533±0.5947
RZ-15-03	5.0002	7.8±0.1	104.8±1.3	17.39±0.00008721	-5.21±2.72	1.907±0.001043	9.065±0.508	18.13±1.02	9.533±0.5947
Quelccaya Ice Cap									
Q-2-03	3.4872	5.5	104.5±1.3	14.74±0.0001008	9.64±2.31	1.641±0.001162	7.643±0.428	21.92±1.23	9.533±0.5947
Q-3-03	3.7742	5.0	111.3±1.4	30.83±0.0000072	11.49±2.05	0.3437±0.0003476	0.9645±0.059	2.56±0.71	9.533±0.5947
Q-4-03	3.5279	9.1	111.1	16.740±0. 0001031	10.92±2.32	1.865±0.001199	9.436±.528	26.75±1.50	9.533±0.5947
Q-80	3.4983	6.3	107.3	969.8 ±0.00005272	9.18±1.92	1.079±0.0006096	4.849±0.272	13.86±0.78	9.533±0.5947
Q-81	3.5603	5.3	108.4	13.48 ±0.00006420	11.16±2.47	1.503±0.000741	7.214±.404	20.26±1.14	9.533±0.5947

[1]Uncertainty reflects long-term lab precision (5.6%; Goehring et al., 2019) based on replicate measurements of the CRONUS-A intercomparison material (Jull et al., 2015), except for sample Q-3-03, for which we use its larger measurement uncertainty.

Table S4. ^{10}Be blank data. All uncertainties are 1σ.

Blank ID	Be Carrier Added (g)	^{9}Be Carrier Concentration (ppm)	$^{10}Be/^{9}Be$[1] (10^{-15})	^{10}Be (10^4 atoms)
BAB_061517	0.2585	1040	8.10±0.76	14.56±1.36
MJ-BL65	0.01285	1337	7.00±0.58	0.80±0.07
MKBL1_Nov07	0.2036	996	0.60±0.19	0.90±0.29
MKBL2_Nov07	0.2039	996	1.32±0.19	1.98±0.28
MKBL1_Nov07 and MKBL2_Nov07			0.96±0.51	

[1]Measured relative to standard 07KNSTD3110 with an assumed $^{10}Be/^{9}Be$ ratio of 2.85 x 10^{-12} (Nishiizumi et al., 2007).

Supplementary References

Balco, G., Stone, J. O., Lifton, N. A., and Dunai, T. J., 2008, A complete and easily accessible means of calculating surface exposure ages or erosion rates from 10Be and 26Al measurements: Quaternary Geochronology, v. 3, p. 174-195.

Borchers, B., Marrero, S., Balco, G., Caffee, M., Goehring, B., Lifton, N., Nishiizumi, K., Phillips, F., Schaefer, J., and Stone, J., 2016, Geological calibration of spallation production rates in the CRONUS-Earth project: Quaternary Geochronology, v. 31, p. 188-198.

Goehring, B. M., Wilson, J., and Nichols, K., 2019, A fully automated system for the extraction of in situ cosmogenic carbon-14 in the Tulane University cosmogenic nuclide laboratory: Nuclear Instruments and Methods in Physics Research Section B: Beam Interactions with Materials and Atoms, v. 455, p. 284-292.

Goehring, B. M., Schaefer, J. M., Schluechter, C., Lifton, N. A., Finkel, R. C., Jull, A. J. T., Akçar, N., and Alley, R. B., 2011, The Rhone Glacier was smaller than today for most of the Holocene: Geology.

Jackson, M. S., Kelly, M. A., Russell, J. M., Doughty, A. M., Howley, J. A., Zimmerman, S. R. H., and Nakileza, B., 2020, Holocene glaciation in the Rwenzori Mountains, Uganda: Clim. Past Discuss., v. 2020, p. 1-38.

Jull, A. J. T., Scott, E. M., and Bierman, P., 2015, The CRONUS-Earth inter-comparison for cosmogenic isotope analysis: Quaternary Geochronology, v. 26, p. 3-10.

Kelly, M. A., Lowell, T. V., Applegate, P. J., Phillips, F. M., Schaefer, J. M., Smith, C. A., Kim, H., Leonard, K. C., and Hudson, A. M., 2015, A locally calibrated, late glacial 10Be production rate from a low-latitude, high-altitude site in the Peruvian Andes: Quaternary Geochronology, v. 26, p. 70-85.

Lifton, N., Sato, T., and Dunai, T. J., 2014, Scaling in situ cosmogenic nuclide production rates using analytical approximations to atmospheric cosmic-ray fluxes: Earth and Planetary Science Letters, v. 386, no. 0, p. 149-160.

Nishiizumi, K., Imamura, M., Caffee, M. W., Southon, J. R., Finkel, R. C., and McAninch, J., 2007, Absolute calibration of 10Be AMS standards: Nuclear Inst. and Methods in Physics Research, B, v. 258, no. 2, p. 403-413.